[4] Seide, P., "On the buckling of truncated conical shells in torsion," J. Appl. Mech. 29, 320–328 (June 1962).

[5] Singer, J., Eckstein, A., and Baruch, M., "Buckling of conical shells under external pressure, torsion, and axial compression," Technion Research and Development Foundation, TAE Rept. 19, TR (Final) Contract AF61(052)-339 (September 1962).

[6] Seide, P., "On the buckling of truncated conical shells under uniform hydrostatic pressure," *Proceedings of the IUTAM Symposium on the Theory of Thin Elastic Shells* (North Holland Publishing Co., Amsterdam, Holland, 1960).

[7] Stein, M., "The effect on the buckling of perfect cylinders of pre-buckling deformations and stresses induced by edge support," *Collected Papers on Instability of Shell Structures—1962*, NASA TN D-1510 (December 1962), pp. 317–327.

[8] Fischer, G., "Uber der Einfluss der gelenkigen Lagerung auf die Stabilität dünnwandiger Kreiszylinderschalen unter Axiallast und Innerdruct," Z. Flugwiss 11, 111–119 (1963); transl. and available as Northrop Corp. Rept. NOR 64-80.

[9] Seide, P., Weingarten, V. I., and Morgan, D. J., "Final report on the development of design criteria for elastic stability of thin shell structure," Space Technology Labs., Rept. STL/TR-60-0000-19425, EM 10-26, Air Force Ballistic Missile Div./TR-61-7 (December 31, 1960).

[10] Weingarten, V. I., "Experimental investigation of the stability of internally pressurized conical shells under torsion," Aerospace Corp. Rept. TDR-269 (4560-40)-1 (1964).

OCTOBER 1964 AIAA JOURNAL VOL. 2, NO. 10

Nonlinear Response of Cylindrical Shells Subjected to Dynamic Axial Loads

ROBERT S. ROTH* AND JEROME M. KLOSNER†
Avco Corporation, Wilmington, Mass.

A study has been made to determine the dynamic instability of long, circular cylindrical shells having initial imperfections subjected to time-dependent axial edge loads. By using a nonlinear shell theory and including the radial inertia terms, equations of the Kármán-Tsien type were derived. Rather than attempt to solve the equations directly, an approximate four-term deflection function having time-dependent coefficients was assumed, and, by applying Hamilton's principle, a system of four coupled, second-order differential equations relating these coefficients was obtained. A numerical-integration scheme was used to solve these equations as a function of five parameters, namely, two initial imperfection parameters, two parameters governing the time-dependent geometrical configuration of the shell (equivalent to selecting the number of waves in the axial and circumferential directions), and the applied axial compressive load. A criterion for the dynamic buckling load of the cylinder has been established, and a study has been made of the magnitude of the critical loads on the shell as a function of the initial imperfections. The effect of applying a load for a short time has revealed that a significant increase in the dynamic buckling stress occurs as the time duration of loading decreases.

Nomenclature

$a_1(t) \ldots a_4(t)$ = coefficients of the assumed deflection shape [Eq. (11)]
c = speed of sound in the material ($c^2 = E/\rho$)
d_1, d_2 = coefficients of the initial deflection shape
D = bending stiffness [$D = Eh^3/12(1 - \nu^2)$]
E = Young's modulus
$F(x, y)$ = Airy stress function
g = average circumferential stress due to average circumferential inertia term [Eq. (13)]
$\bar{g}$ = nondimensional average circumferential stress $\bar{g} = (gR/Eh)$
h = shell thickness
$\bar{I}$ = nondimensional impulse
$\bar{I}_B$ = nondimensional critical impulse
L = shell length
m, n = number of axial and circumferential waves, respectively
R = mean shell radius
t = time
T = kinetic energy of the shell
u, v = axial and circumferential radial displacements of the median surface, respectively
V_1, V_2, V_3 = extensional strain energy, bending strain energy, and potential of applied axial loads, respectively
w = inward radial displacement of the median surface
$\bar{w}$ = initial inward radial displacement
w^* = total inward radial displacement ($w^* = w + \bar{w}$)
x, y = axial and circumferential coordinates on median surface of shell, respectively
α = geometrical parameter ($\alpha = \lambda_y^2/\pi^2 Rh$)
β = geometrical parameter ($\beta = \lambda_y/\lambda_x$)
$\gamma_{xy}, \epsilon_x, \epsilon_y$ = median surface shear, axial, and circumferential strains, respectively
ϵ = unit end shortening of shell
λ_x, λ_y = half-wavelengths in the axial and circumferential directions, respectively
ν = Poisson's ratio
ρ = mass density of shell material
σ = applied average axial compressive stress
$\bar{\sigma}$ = nondimensional applied average compressive stress $\bar{\sigma} = (\sigma R/Eh)$

Presented as Preprint 64-76 at the AIAA Aerospace Sciences Meeting, New York, January 20–22, 1964; revision received July 1, 1964. This study was sponsored in part by the U. S. Air Force under Contract AF04(694)-239 with the Avco Corporation.

* Staff Scientist. Member AIAA.

† Consultant; also Associate Professor of Applied Mechanics, Polytechnic Institute of Brooklyn, Brooklyn, N. Y. Member AIAA.

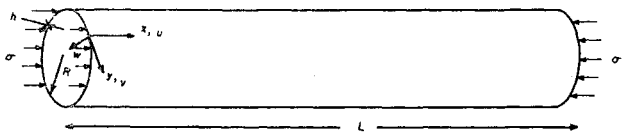

Fig. 1 Shell geometry.

$\bar{\sigma}_B$ = nondimensional dynamic buckling stress
σ_{cr} = critical stress
σ_x, σ_y, τ_{xy} = axial, circumferential, and shear median surface stresses, respectively
τ = nondimensional time ($\tau = ct/R$)
$\bar{\tau}$ = nondimensional time duration of loading
∇^4 = biharmonic operator [$\nabla^4 = (\partial^4/\partial x^4) + 2(\partial^4/\partial x^2\partial y^2) + (\partial^4/\partial y^4)$]
$(\ )_{,x}$ = $\partial(\ )/\partial x$
$(\dot{\ })$ = $\partial(\ )/\partial\tau$

Introduction

RESEARCH concerned with the elastic stability of circular cylindrical shells has been carried on by many authors since the early nonlinear investigations by Donnell[1] and Kármán and Tsien.[2] The latter investigation pointed out the way to explain the large discrepancy between experimental results and the classical buckling loads. An excellent discussion of these investigations as well as a report on some current work can be found in an article by Thielemann.[3] However, all of these past efforts have been limited to a quasistatic analysis, and it has been tacitly assumed that the loads or deformations are slowly applied.

With the advent of missile structures, many new problem areas have arisen. One of these concerns itself with the dynamic response of shell structures. Consequently, several papers have recently appeared in which the dynamic buckling of shells has been investigated.

Bolotin[4] investigated the dynamic stability of circular, cylindrical, and spherical shells using infinitesimal deflection theory. A similar investigation was done by Wood and Koval[5] and was concerned with an experimental and analytical investigation of the collapse of thin-walled cylindrical shells under various loading conditions. These analyses were improved upon by Agamirov and Vol'mir[6] by use of finite-deflection theory. The longitudinal inertia as well as the average circumferential stress arising from the inertia of the shell were neglected in their formulation. Furthermore, by making certain restrictions on the time-dependent coefficients of the assumed radial-deflection function, the system of equations was reduced to one having one degree of freedom. Kadashevich and Pertsev[7] improved the previous analysis by including the inertia induced average circumferential stress and by using a less restricted deflection function, thereby resulting in a system of equations having three degrees of freedom. Only typical response curves were presented for suddenly applied, uniformly distributed transverse loads of constant magnitude and transient and prolonged duration, and for uniformly distributed transverse loads increasing linearly with time. Coppa and Nash[8] used a similar analysis to investigate the dynamic buckling of cylindrical shells subject to longitudinal loads increasing with time. Their system of equations was reduced to a set having two degrees of freedom. The investigation of a clamped, shallow spherical cap subjected to a time-dependent load has been investigated by Budiansky and Roth[9] and Roth.[10] The buckling load was defined to be the load at which a large increase in the amplitudes of the average deflections was seen to occur.

This paper is the result of an investigation concerned with the instability of circular cylindrical shells subjected to uniformly distributed, suddenly applied axial loads of constant magnitude, and of prolonged or finite-time duration. The longitudinal inertia term is neglected, and the resulting system of equations is reduced to a set having four degrees of freedom. The buckling criterion used is similar to that used by Budiansky and Roth (i.e., the load at which a large increase in the amplitudes of the deflection occurs).

Analytical Formulation

The physical problem considered is the determination of the response of a long, circular cylindrical shell, having initial imperfections, to an arbitrary time-dependent axial edge load. A nonlinear large deflection shell theory is used in the development of a criterion for dynamic instability. Although the analysis and the numerical program developed allow for any arbitrary variation of end loading with time, for the purpose of the present study, the loading was taken to be in the form of a Heaviside step function in time.

The geometry of the system is defined in Fig. 1, where u, v, and w are the axial, circumferential, and radial displacements of the median surface, respectively. It is assumed throughout the study that the shell is stressed elastically and is of a sufficient length so that the effect of the edge restraints is negligible. It has been shown that this assumption is valid if the length of the shell is greater than 1.5 times its radius [see, for example, Eq. (1)].

Median Surface Strains and Displacements

The median surface nonlinear strain-displacement relationships for thin, circular cylindrical shells of radius R, having an initial imperfection $\bar{w}$, are based on the work of Donnell.[1] They are

$$\begin{aligned} \epsilon_x &= u_{,x} + \tfrac{1}{2}(w_{,x})^2 + \bar{w}_{,x}w_{,x} \\ \epsilon_y &= v_{,y} - (w/R) + \tfrac{1}{2}(w_{,y})^2 + \bar{w}_{,y}w_{,y} \\ \gamma_{xy} &= u_{,y} + v_{,x} + w_{,x}\,w_{,y} + \bar{w}_{,x}\,w_{,y} + \bar{w}_{,y}\,w_{,x} \end{aligned} \tag{1}$$

The axial, circumferential, and shear stresses in the median surface are given in terms of the median surface strains by the usual form of Hooke's law for thin shells:

$$\begin{aligned} \sigma_x &= [E/(1-\nu^2)](\epsilon_x + \nu\epsilon_y) \\ \sigma_y &= [E/(1-\nu^2)](\epsilon_y + \nu\epsilon_x) \\ \tau_{xy} &= [E/2(1+\nu)]\gamma_{xy} \end{aligned} \tag{2}$$

where σ_x and σ_y are positive in tension, E is the modulus of elasticity, and ν ($= 0.3$) is Poisson's ratio. A comma placed after a function denotes differentiation with respect to the coordinate [$\partial/\partial x = (\ )_{,x}$].

Kinetic and Potential Energy

The elastic, extensional strain energy corresponding to the median surface stresses is

$$V_1 = \frac{h}{2E}\int_0^L\int_0^{2\pi R} [(\sigma_x + \sigma_y)^2 - 2(1+\nu)(\sigma_x\sigma_y - \tau_{xy}^2)]dxdy \tag{3}$$

where h is the wall thickness of the shell, R its radius, and L its length. The elastic, bending strain energy of the shells is given as

$$V_2 = \frac{D}{2}\int_0^L\int_0^{2\pi R} [(w_{,xx} + w_{,yy})^2 - 2(1-\nu)(w_{,xx}w_{,yy} - w_{,xy}^2)]dxdy \tag{4}$$

in which the bending stiffness

$$D = Eh^3/[12(1-\nu^2)]$$

The potential energy of the applied axial load can be expressed as

$$V_3 = -h\int_0^{2\pi R} \sigma_x\Big|_{x=L} dy \int_0^L u_{,x}\,dx \tag{5}$$

Finally, the expression for the kinetic energy of the shell can be written as

$$T = \frac{1}{2}\rho h \int_0^L \int_0^{2\pi R} \left(\frac{\partial w}{\partial t}\right)^2 dy\, dx \tag{6}$$

where ρ is the mass density of shell material, and t denotes time. It should be noted that the axial inertia terms are neglected.

Equations of Motion

The equations of motion are found by applying Hamilton's principle. The total energy, considered as an implicit function of the displacements, is made stationary by setting the total variation with respect to u, v, and w equal to zero. The resulting three equations are

$$(D/h)\nabla^4 w = -\rho w_{,tt} + (\sigma_x w_{,x}{}^*)_{,x} + (\tau_{xy} w_{,x}{}^*)_{,y} + (\tau_{xy} w_{,y}{}^*)_{,x} + (\sigma_y w_{,y}{}^*)_{,y} + (\sigma_y/R) \tag{7a}$$

where

$$w^* = w + \bar{w} \tag{7b}$$

and

$$\sigma_{x,x} + \tau_{xy,y} = 0 \qquad \tau_{xy,x} + \sigma_{y,y} = 0 \tag{7c}$$

The last two equations of (7) can be satisfied identically by introducing an Airy stress function F defined as follows:

$$\begin{aligned} \sigma_x &= F_{,yy} \\ \sigma_y &= F_{,xx} \\ \tau_{xy} &= -F_{,xy} \end{aligned} \tag{8}$$

Thus, the first equilibrium equation can now be rewritten as

$$(D/h)\nabla^4 w = -\rho w_{,tt} + F_{,yy} w_{,xx}{}^* - 2F_{,xy} w_{,xy}{}^* + F_{,xx} w_{,yy}{}^* + (1/R)F_{,xx} \tag{9}$$

The compatibility equation is given as[1]

$$\nabla^4 F = E[(w_{,xy})^2 - w_{,xx}w_{,yy} - (1/R)w_{,xx} + 2\bar{w}_{,xy}w_{,xy} - \bar{w}_{,yy}w_{,xx} - \bar{w}_{,xx}w_{,yy}] \tag{10}$$

where

$$\nabla^4 = (\ )_{,xxxx} + 2(\ )_{,xxyy} + (\ )_{,yyyy}$$

The mathematical problem then resolves itself to solving two nonlinear differential equations, (9) and (10), for the stress function F and the inward radial displacement w, subject to the appropriate boundary and initial conditions.

Approximate Displacement Function and Initial Deformation

Rather than attempt to solve this set of equations directly a technique was used whereby approximate functions for w and $\bar{w}$ were substituted into the compatibility equation (10) to find F. Subsequent solution of Eq. (9) was obtained by means of a Ritz-Galerkin method, or by the application of Hamilton's principle. This led to a set of ordinary, nonlinear differential equations which were solved by numerical methods on the IBM 7094 digital computer.

The approximate radial deflection function was chosen to have the following form:

$$w = h\left[a_1(t)\cos\frac{\pi x}{\lambda_x}\cos\frac{\pi y}{\lambda_y} + a_2(t)\cos\frac{2\pi x}{\lambda_x} + a_3(t)\cos\frac{2\pi y}{\lambda_y} + a_4(t)\right] \tag{11}$$

where a_1 through a_4 are functions of time, and λ_x and λ_y are the half-wavelengths in the axial and circumferential directions, respectively.

This form is identical to that used by Kempner[11] for a static analysis and represents both the symmetric and unsymmetric components of the radial deflection. Equation (11) corresponds to a shell whose ends are neither clamped nor simply supported (since the a_4 term represents a uniform expansion or contraction of the shell); however, as has been pointed out in the past, the boundary conditions on the displacements are insignificant if the shell's length is sufficient. Combined, the foregoing modes allow for the familiar diamond-shaped buckling form occurring so often in experiments. The initial imperfections of the shell were chosen to be

$$\bar{w} = h\left(d_1\cos\frac{\pi x}{\lambda_x}\cos\frac{\pi y}{\lambda_y} + d_2\cos\frac{2\pi x}{\lambda_x}\right) \tag{12}$$

Stress Function

The substitution of the expression for w and $\bar{w}$ [Eqs. (11) and (12)] into the compatibility equation (10) results in the following solution for the stress function F:

$$F = b_1\cos\frac{3\pi x}{\lambda_x}\cos\frac{\pi y}{\lambda_y} + b_2\cos\frac{\pi x}{\lambda_x}\cos\frac{3\pi y}{\lambda_y} + b_3\cos\frac{2\pi x}{\lambda_x}\cos\frac{2\pi_y}{\lambda_y} + b_4\cos\frac{\pi x}{\lambda_x}\cos\frac{\pi_y}{\lambda_y} + b_5\cos\frac{2\pi x}{\lambda_x} + b_6\cos\frac{2\pi y}{\lambda_y} - \frac{1}{2}\sigma y^2 + \frac{1}{2}gx^2 \tag{13}$$

where

$$b_1 = -\left[\frac{2h^2E\beta^2}{(9\beta^2+1)^2}\right](a_1a_2 + a_1d_2 + a_2d_1)$$

$$b_2 = -\left[\frac{2h^2E\beta^2}{(\beta^2+9)^2}\right](a_1a_3 + a_3d_1)$$

$$b_3 = -\left[\frac{Eh^2\beta^2}{(\beta^2+1)^2}\right](a_2a_3 + a_3d_2)$$

$$b_4 = -\left[\frac{2Eh^2\beta^2}{(\beta^2+1)^2}\right]\left(a_1a_3 + a_1a_2 - \frac{\alpha}{2}a_1 + a_1d_2 + a_2d_1 + a_3d_1\right)$$

$$b_5 = -\left(\frac{Eh^2}{16\beta^2}\right)\left(\frac{a_1{}^2}{2} + a_1d_1 - 4\alpha a_2\right)$$

$$b_6 = -\left(\frac{Eh^2\beta^2}{32}\right)(a_1{}^2 + 2a_1d_1)$$

and

$$\beta = \lambda_y/\lambda_x \qquad \alpha = \lambda_y{}^2/\pi^2Rh \tag{14}$$

The terms σ and g represent the average applied axial compressive stress and the average circumferential stress (arising as a result of the average radial acceleration), respectively.

Determination of the Average Circumferential Stress g and the Unit End Shortening

If the condition is now imposed that the circumferential displacement v must be periodic, which is mathematically stated as

$$\int_0^{2\pi R} v_{,y}dy = \int_0^{2\pi R}\left\{\frac{1}{E}(F_{,xx} - \nu F_{,yy}) + \frac{w}{R} - \frac{1}{2}(w_{,y})^2 - \bar{w}_{,y}w_{,y}\right\}dy = 0 \tag{15}$$

the following expression is obtained for $\bar{g}$ in terms of the deflection parameters:

$$\bar{g} = \frac{1}{4\alpha}\left(\frac{1}{2}a_1^2 + 4a_3^2 + a_1d_1\right) - a_4 - \nu\bar{\sigma} \tag{16}$$

where

$$\bar{\sigma} = \sigma R/Eh \qquad \bar{g} = gR/Eh \tag{17}$$

The unit end shortening can be obtained as follows:

$$\epsilon = -\frac{1}{L}\int_0^L u_{,x}\,dx$$

$$= -\frac{1}{L}\int_0^L \left[\frac{1}{E}(F_{,yy} - \nu F_{,xx}) - \frac{1}{2}(w_{,x})^2 - \bar{w}_{,x}w_{,x}\right]dx \tag{18}$$

The substitution of Eqs. (11–13) into Eq. (18) yields

$$\left(\frac{\epsilon R}{h}\right) = \bar{\sigma} + \nu\bar{g} + \frac{\beta^2}{8\alpha}(a_1^2 + 2a_1d_1 + 8a_2^2 + 16a_2d_2) \tag{19}$$

Nonlinear Differential Equations

Upon substituting the expressions for F, w, and $\bar{w}$ into Eqs. (3–6) and applying Hamilton's principle, the following set of four simultaneous nonlinear differential equations is obtained:

$$\frac{1}{2}\ddot{a}_1 + \left[\frac{(1+\beta^2)^2}{24\alpha^2(1-\nu^2)} - \frac{\beta^2\bar{\sigma}}{2\alpha}\right]a_1 +$$
$$2B_1(a_1a_2 + a_1d_2 + a_2d_1)(a_2 + d_2) + 2B_2a_3^2(a_1 + d_1) +$$
$$2B_4\left(\frac{1}{2}a_1^2 + a_1d_1 - 4\alpha a_2\right)(a_1 + d_1) +$$
$$4B_5(a_1^2 + 2a_1d_1)(a_1 + d_1) + \frac{\bar{g}}{2\alpha}(a_1 + d_1) +$$
$$2B_3\left(a_1a_3 + a_1a_2 - \frac{\alpha}{2}a_1 + a_1d_2 + a_2d_1 + a_3d_1\right)\times$$
$$\left(a_2 + a_3 - \frac{\alpha}{2} + d_2\right) = \frac{\beta^2\bar{\sigma}}{2\alpha}d_1 \tag{20}$$

$$\ddot{a}_2 + \left(\frac{4\beta^4}{3\alpha^2(1-\nu^2)} - \frac{4\beta^2}{\alpha}\bar{\sigma}\right)a_2 + 2B_1(a_1a_2 + a_1d_2 + a_2d_1)\times$$
$$(a_1 + d_1) + 8B_3a_3^2(a_2 + d_2) -$$
$$8\alpha B_4\left(\frac{1}{2}a_1^2 + a_1d_1 - 4\alpha a_2\right) +$$
$$2B_3\left(a_1a_3 + a_1a_2 - \frac{\alpha}{2}a_1 + a_1d_2 + a_2d_1 + a_3d_1\right)\times$$
$$(a_1 + d_1) = 4\frac{\beta^2}{\alpha}\bar{\sigma}d_2 \tag{21}$$

$$\ddot{a}_3 + \left[\frac{4}{3\alpha^2(1-\nu^2)}\right]a_3 + 2B_2a_3(a_1 + d_1)^2 +$$
$$8B_3a_3(a_2 + d_2)^2 + 2B_3\left(a_1a_3 + a_1a_2 - \frac{\alpha}{2}a_1 + a_1d_2 +\right.$$
$$\left.a_2d_1 + a_3d_1\right)(a_1 + d_1) + \frac{4\bar{g}}{\alpha}a_3 = 0 \tag{22}$$

$$\ddot{a}_4 + a_4 = -\nu\bar{\sigma} + \frac{1}{4\alpha}\left[\frac{1}{2}a_1^2 + 4a_3^2 + a_1d_1\right] \tag{23}$$

where the nondimensional time is defined as

$$\tau = (c/R)t$$
$$c^2 = (E/\rho) \tag{24}$$
$$(\dot{}) = \partial(\ )/\partial\tau$$

Also,

$$B_1 = \frac{(\beta^4/\alpha^2)}{(9\beta^2+1)^2} \qquad B_2 = \frac{(\beta^4/\alpha^2)}{(\beta^2+9)^2}$$
$$B_3 = \frac{(\beta^4/\alpha^2)}{(\beta^2+1)^2} \qquad B_4 = \frac{1}{32\alpha^2} \tag{25}$$
$$B_5 = \frac{(\beta^4/\alpha^2)}{128}$$

Comparison of Eqs. (16) and (23) reveals that $\bar{g} = \ddot{a}_4$. This is no surprise, since $\bar{g}$ is the nondimensional average circumferential stress that must arise from the average radial inertia expression.

A unique solution of Eqs. (20–23) can be obtained if the initial displacements and velocities of a_1 through a_4 are specified. The solution of this set depends on five parameters, i.e., d_1 and d_2 (the initial imperfections of the cylindrical shell), α and β (the parameters governing the geometrical configuration of the shell), and $\bar{\sigma}$ (the applied axial compressive stress).

Numerical Analysis

The set of four simultaneous nonlinear ordinary differential equations (20–23) plus eight given initial conditions defines the initial value problem of which a mathematical solution is sought.

These equations have been numerically solved as functions of the five parameters (α, β, $\bar{\sigma}$, d_1, and d_2) by use of the Runge-Kutta formula.[12]

Discussion of the Parameters

Load parameter $\bar{\sigma}(\tau)$

Although the preceding analytical development allows one to consider an axial end load varying arbitrarily with time, the present numerical study will be limited to consideration of loads having a step-function variation in time and acting for finite- or infinite-time intervals.

The nondimensional time duration of loading will be denoted by $\bar{\tau}$. Thus, the magnitude of the step and the interval of its duration will be the only load parameters used in this problem.

Geometrical parameters

The geometrical parameters α and β are defined as

$$\alpha = \lambda_y^2/\pi^2Rh \qquad \beta = \lambda_y/\lambda_x \tag{26}$$

where the half-wavelengths are taken as

$$\lambda_x = L/2m \qquad \lambda_y = \pi R/n \tag{27}$$

and m and n are the number of axial and circumferential waves, respectively. For arbitrarily chosen values of m and n, the dynamic critical load may be obtained. However, it is necessary to find the minimum critical load, since this minimum dynamic critical load is chosen to be the dynamic buckling load of the cylindrical shell. In the calculations presented, the initial imperfection d_1 has been taken to be 1.0, 0.5, and 0.1, while $d_2 = 0$.

Discussion of the Results

The results of the current study are presented in Figs. 2 to 8 and indicate the response to an axial load, suddenly applied to the cylinder, held constant for a given time $\bar{\tau}$, and then removed. Three types of loads were investigated, namely, those having a long-time duration (i.e., long in comparison to time at which the first maximum of shell response

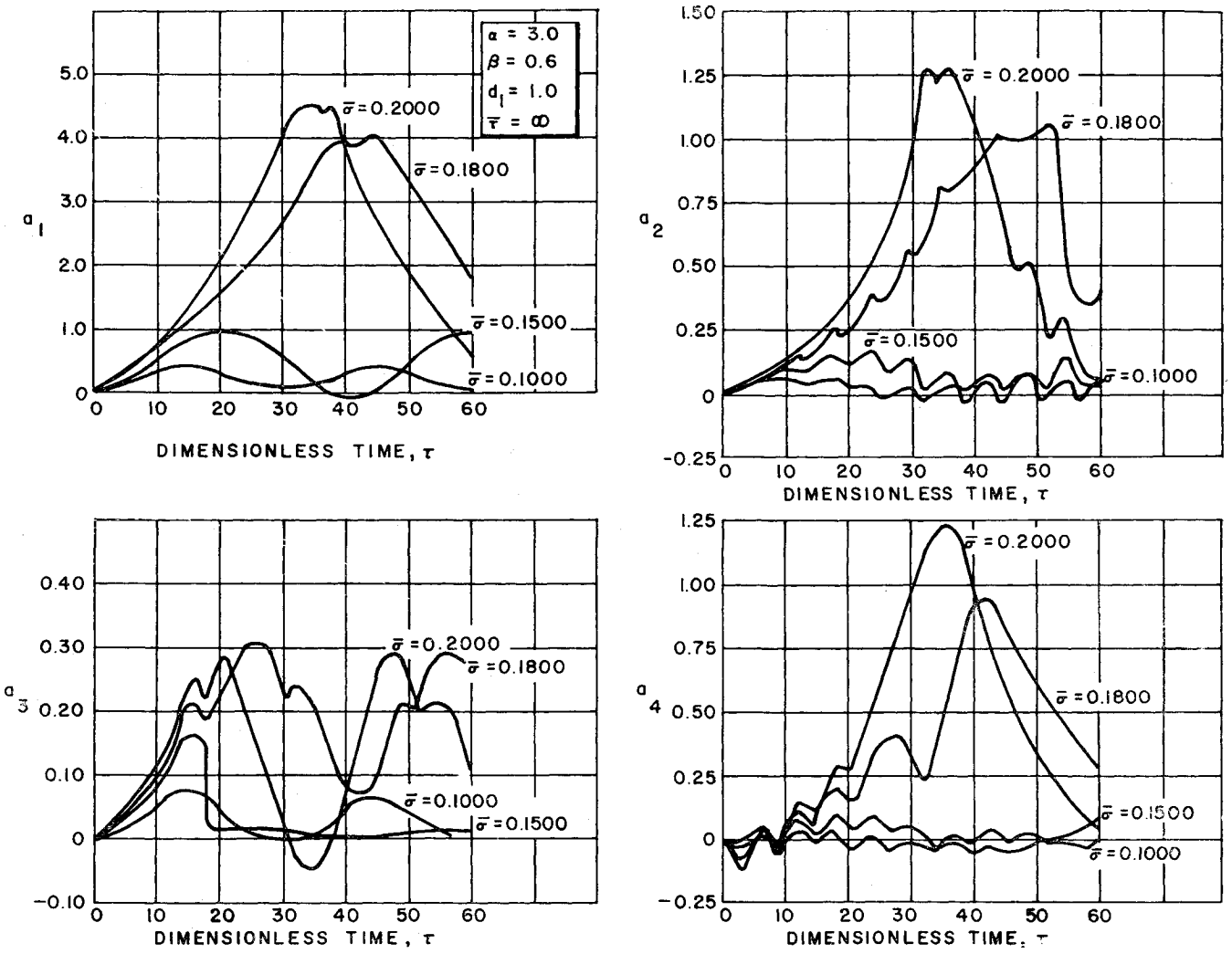

Fig. 2 Response of the deformation mode to axial stress.

occurs), short-time-duration loads (i.e., those having time durations that are less than the time at which first maximum occurs), and an impulsive radial load, inducing initial radial (a_1 mode) velocities. The response of the cylinder to a long-time duration loading will be studied thoroughly, whereas the response to both short-time durations and impulse loads will be considered briefly.

Typical numerical results of the solution of the set of coupled nonlinear differential equations to a loading of long-time duration are shown in Fig. 2, where the time histories

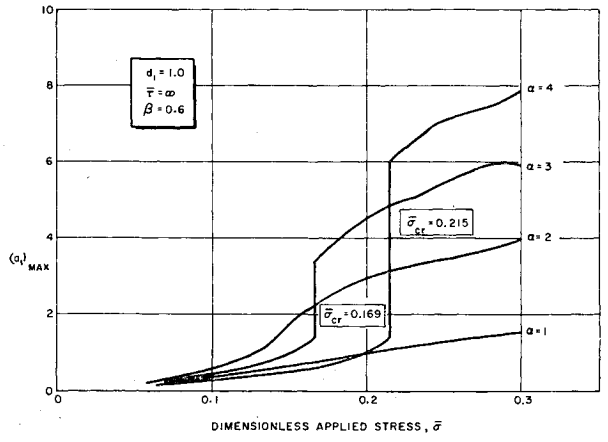

Fig. 3 Variation of $(a_1)_{max}$ with stress (determination of the critical stress).

of each of the four assumed modes of deformation are presented for several values of the applied stress. It should be noted that these results are for values of the initial imperfections of $d_1 = 1.0$, $d_2 = 0.0$ and for the geometrical parameters $\alpha = 3$ and $\beta = 0.6$. The numerical solution of the set of differential equations was begun by assuming a set of initial conditions on all four modes.

By considering the behavior of the response of the a_1 mode only, it can be seen from Fig. 2 that, as the load $\bar{\sigma}$ increases, the time to the first maximum increases, until a certain load is reached, after which the time to first maximum decreases. Associated with the reversal in the trend of the time to first maximum, the magnitude of a_1 takes a sudden jump in value. At this load, the behavior of the structure is changing radically. If the magnitude of the first maximum of a_1 is plotted against the applied load, then this sudden change is seen clearly and is shown in Fig. 3. The load at which this sudden change occurs will be called the critical load, associated with a given set of geometrical parameters and initial imperfections. It has been found that the variation of the unit end shortening follows essentially the same nonlinear behavior as the a_1 mode. Thus, establishing an instability criterion by investigating the response of only the a_1 mode is justified.

As was mentioned earlier in the paper, the choice of geometrical parameters α and β, which is equivalent to selecting the number of waves in the axial and circumferential directions, may result in large critical loads; hence, it is necessary to examine the critical loads over a range of α and β and determine the minimum critical load. The typical results of this study are shown in Fig. 4 for the value of initial imper-

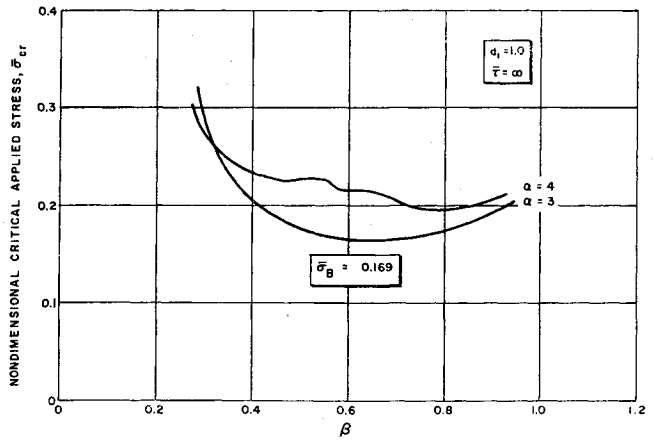

Fig. 4 Variation of critical stress with geometrical parameters $d_1 = 1.0$ (determination of the dynamic buckling stress—minimum critical stress).

fection $d_1 = 1.0$. The minimum critical load obtained was defined as the nondimensional dynamic buckling stress of the cylinder $\bar{\sigma}_B$.

The variation of the dynamic buckling stress of the cylinder with the initial imperfection is an important result of the study (see Fig. 5). For the case of zero imperfections, it was found that the dynamic buckling stress coincided with that obtained from the classical linear theory. The calculations for this case were carried out by setting the initial imperfections d_1 and d_2 equal to zero in the set of nonlinear equations (20–23) and choosing initial conditions corresponding to either a slightly displaced shell [$a_1(0) = 0.001$] or one having a small initial velocity [$\dot{a}_1(0) = 0.001$].

The early static studies of a cylinder under an axial compression, carried out by Kármán and Tsien,[2] indicated that a buckled cylinder could be maintained in equilibrium under an axial stress considerably below the classical buckling stress. Furthermore, it was observed that the classical buckling load predicted was much higher (by a factor of 3) than that observed in the laboratory. It was then postulated that this type of buckling is very sensitive to imperfections and disturbances. Intuitively, Donnell and Wan[13] pointed out that the effect of accidental lateral loadings on the peak resistance of the cylinder is small and that the most important factors influencing the resistance are the initial imperfections, initial stresses, and deviations from uniform, isotropic-elastic behavior.

In the present dynamic study of an initially perfect shell, it was found that, when a small initial displacement or a small initial velocity was assumed, a sudden jump in the amplitude of the a_1 mode did not occur until the stress reached a value equal to the classical buckling stress ($\bar{\sigma} = 0.605$). This indicates that a significant potential barrier exists between the prebuckling and postbuckling portions of the static-equilibrium curves.[11] Thus, it is suggested that a perfect cylinder will not become unstable until the end load reaches the linear buckling load unless a large lateral dynamic disturbance occurs see (Figs. 6 and 7) and that the initial imperfections play a dominant role in the reduction of peak stresses (see Fig. 5). Recent experimental work,[14] using carefully constructed almost-perfect cylinders, has shown that the high classical buckling load can be approached.

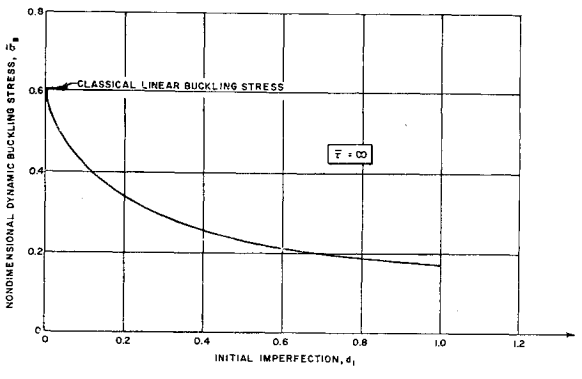

Fig. 5 Variation of the nondimensional dynamic buckling stress ($\bar{\sigma}_B$) with initial imperfections.

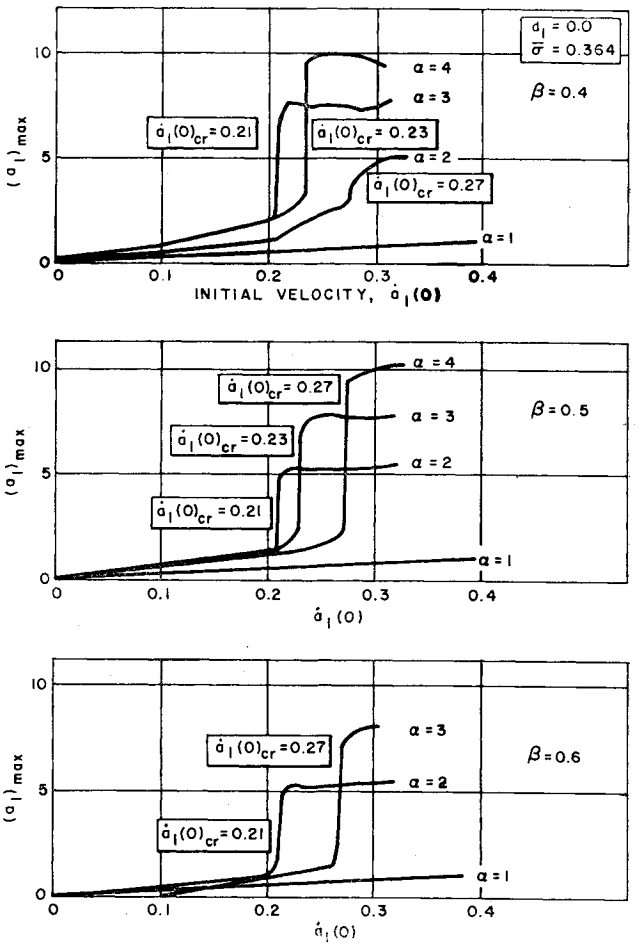

Fig. 6 Variation of $(a_1)_{max}$ with initial velocity.

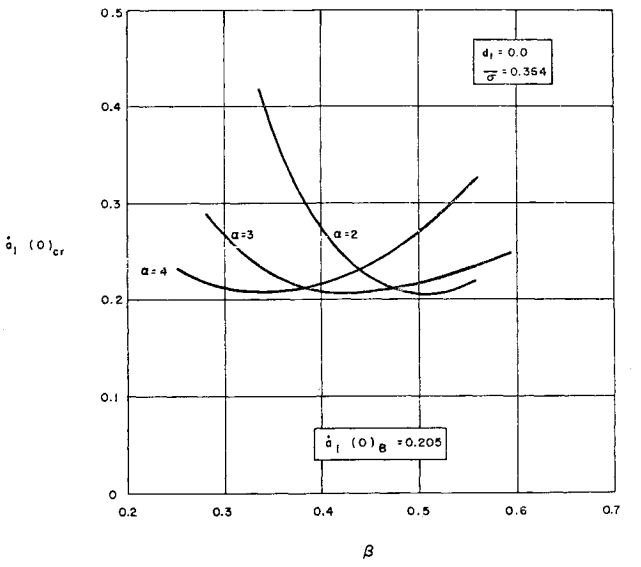

Fig. 7 Variation of critical initial velocity with geometrical parameters.

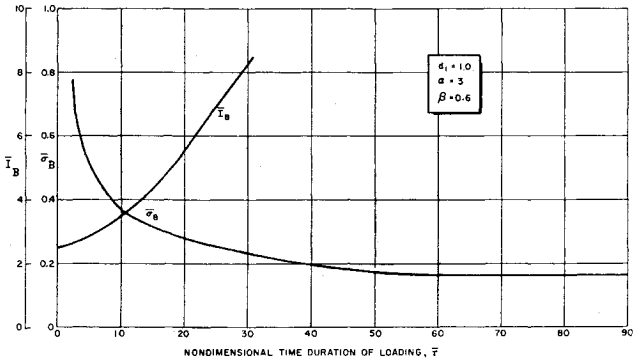

Fig. 8 Variation with load duration of nondimensional dynamic buckling stress and critical impulse.

The result of an investigation concerned with the effects of lateral disturbances on stability of a cylinder with no initial imperfections is shown in Figs. 6 and 7. Here, it has been assumed that an initially perfect cylinder has been subjected to some disturbances that have given an initial velocity to the a_1 mode.

Finally, the result of a study concerned with the effect of the time duration of loading $\bar{\tau}$ of the dynamic buckling load is presented in Fig. 8. The results are presented for a shell having the same geometrical parameters as used in obtaining the dynamic buckling stress of a shell having an initial imperfection $d_1 = 1.0$, subjected to a load of infinite-time duration. It can be seen that the dynamic buckling stress decreases with an increase of the time duration of loading and that no further decrease occurs after $\bar{\tau} = 60$, which is the time of occurrence of first maximum for a load of infinite-time duration. The critical impulse $\bar{I}_B = \bar{\sigma}_B\bar{\tau}$ decreases as the time duration of loading decreases. Its value at $\tau = 0$ was obtained by relating the impulse to the initial velocities by using Eqs. (20–23).

Conclusions

This paper has been concerned with the dynamic response of a circular cylindrical shell when subjected to a time-dependent axial compressive load. A criterion for the dynamic buckling load of the cylinder has been established, and a study has been made of the critical loads on the shell for different initial imperfections when the load is applied to the shell for a long period of time. It has been found that the critical load is highly dependent on the initial imperfections, and little effect is found from small outside disturbances.

The effect of applying a load over a short time has been studied, and a significant increase in the dynamic buckling stress with a reduction of time duration of loading has been observed.

References

[1] Donnell, L. H., "A new theory for the buckling of thin cylindrical shells under axial compression and bending," Trans. Am. Soc. Mech. Engrs. **56**, 795–806 (1934).

[2] von Kármán, T. and Tsien, H. S., "The buckling of thin cylindrical shells under axial compression," J. Aeronaut. Sci. **8**, 303–312 (1941).

[3] Thielemann, W. F., *New Developments in the Non-Linear Theories of the Buckling of Thin Cylindrical Shells* (Pergamon Press, New York, 1961), pp. 76–121.

[4] Bolotin, V. V., "Dynamic stability of shells," *Dynamic Stability of Elastic Systems* (Gostekhteoretizdat, Moscow, 1956), Chap. 22; transl. by M. I. Yarymovych as Avco RAD-TR-61-3 (March 1961).

[5] Wood, J. D. and Koval, L. R., "Buckling of cylindrical shells under dynamic loads," AIAA J. **1**, 2576–2582 (1963).

[6] Agamirov, V. L. and Vol'mir, A. S., "Behavior of cylindrical shells under dynamic loading by hydrostatic pressure or by axial compression," ARS J. **31**, 98–101 (1961).

[7] Kadashevich, Y. I. and Pertsev, A. K., "Loss of stability of a cylindrical shell under dynamic loads," ARS J. **32**, 140–142 (1962).

[8] Coppa, A. P. and Nash, W. A., "Dynamic buckling of shell structures subject to longitudinal impact," Aeronautical Systems Div. TDR-62-774 (December 1962).

[9] Budiansky, B. and Roth, R. S., "Axisymmetric dynamic buckling of clamped shallow spherical shells," NASA TN-D-1510 (1962).

[10] Roth, R. S., "Dynamic instability of shallow spherical shells subjected to pressure pulse loading," Avco RAD-TM-62-24 (May 1962).

[11] Kempner, J., "Postbuckling behavior of axial compressed circular cylindrical shells," J. Aeronaut. Sci. **21**, 329–335 (1954).

[12] Crandall, S. H., *Engineering Analysis—A Survey of Numerical Procedures* (McGraw-Hill Book Co., Inc., New York, 1956), Chap. 3, pp. 174–178.

[13] Donnell, L. H. and Wan, C. C., "Effect of imperfections on buckling of thin cylinders and columns under axial compression," J. Appl. Mech. **17**, 73–83 (1950).

[14] Tennyson, R. C., "A note on the classical buckling load of circular cylindrical shells under axial compressions," AIAA J. **1**, 475–476 (1963).